Investigating Lubrication Mechanisms for Silicon Nitride Sliding on Steel: A Multifaceted Study

Nagraj Patil[1], Archana Verma[2], Gaurav Shukla[3], Dr. Shweta Loonkar[4]

[1]Associate Professor, Department of Mechanical Engineering, Faculty of Engineering and Technology, JAIN (Deemed-to-be University), Ramanagara District, Karnataka - 562112, India, Email Id: nagaraj.patil@jainuniversity.ac.in, Orcid Id-0000-0002-5499-0949.
[2]Assistant Professor, Master of Computer Applications, Noida Institute of Engineering and Technology, Greater Noida, Uttar Pradesh, India, Email Id- archanaverma.mca@niet.co.in, Orcid Id- 0000-0002-1539-4642.
[3]Assistant Professor , Maharishi School of Engineering & Technology, Maharishi University of Information Technology, Uttar Pradesh, India, Email Id- gaur.knit@gmail.com, Orcid Id- 0000-0001-7094-9797.
[4]Assitant Professor, Department of ISME, ATLAS SkillTech University, Mumbai, Maharashtra, India, Email Id- , shweta.loonkar@atlasuniversity.edu.in, Orcid Id- 0000-0001-8227-5937.

Electric Motors (EMs) containing lubricated bearings must adhere to a variety of operational specifications and related microenvironments. Lubricate products need to perform under these circumstances. The wear and friction of silicon nitride (〖Si〗_3 N_4) sliding over toughened chrome steel (52100) were used to measure the tribological effectiveness of three commercially available EM lubricates. The EM lubricates that were examined and comparable viscosity ratings; however, they differed in the proportions of lithium or poly-urea thickener to mineral or synthetic base oil (BO). A variety of surface roughness (SR) levels and temperatures were measured to observe behaviour under various lubrication regimes. The results made possible to compare commercially available solutions directly across a range of application-relevant standards and the analysis techniques created as a foundation for upcoming research on the efficiency of EM lubricate.

Keywords: Electric motor (EM), lubricate, wear and friction, lubrication regimes, surface roughness (SR)..

1. Introduction

In the dynamic field of materials science and engineering, researchers are actively investigating new materials and lubricating techniques to improve the efficiency and durability of mechanical devices (Zhang et al 2020). A fascinating field of research involves

examining the relationship between Si_3N_4 and steel surfaces in sliding operations. This is a crucial factor in a wide range of industrial operations, including automobile components and modern machinery (Guo et al 2018). Obtaining an extensive knowledge of the lubricating mechanisms involved in these interactions is crucial for maximizing performance, reducing wear and prolonging the lifespan of mechanical elements (Li and Guo 2018). Technologies involving sliding across steel surfaces have shown great potential for Si_3N_4 due to its extraordinary hardness, chemical inertness and resilience at high temperatures (Lin et al 2020). The combined use of Si_3N_4 and steel presents a promising solution to the difficulties presented by conventional materials, such as the flaw of steel-on-steel interactions to corrosion and wear (Lin et al 2019). The efficacy of the sliding mechanisms is highly dependent on the adoption of appropriate lubricating mechanisms (Elsheikh et al 2020).

The tribological performance of these materials is affected by variables such as roughness of the surface, contacting stress and speed of sliding (Kronberger and Brenner 2023). Evaluating these factors is essential for understanding the intricate interaction between the components during sliding, providing knowledge about phenomena like wear, friction and surface damage (Zhang et al 2019). The lubrication regimes can vary from border lubrication, characterized by substantial direct contact with surface irregularities, to mixed and dynamic lubrication, where a lubricant coating is present to minimize wear and friction (Lee et al 2021). Examining the shift between these lubrication regimes offers an essential understanding of the circumstances in which Si_3N_4 and steel can attain optimal effectiveness and lifespan (He et al 2018). The tribological efficacy of three commercially available EM lubricates was assessed using the wear and friction of Si_3N_4 sliding over hardened steel.

Wang et al (2018) entailed the creation of a novel rolling-sliding contacting device, which utilized an altered pin-on-disk test fixture. The objective was to examine the tribological characteristics of the Si_3N_4/GCr15 tribo-pair across various loads in a rolling-sliding state. Chen et al (2018) examined the feasibility of using Si_3N_4-based composites-metal as an element for sliding pairs in seawater. Specifically, their study focused on analyzing the friction and wear characteristics of Si_3N_4-hBN combinations. Li et al (2022) investigated the friction and wear characteristics of Si_3N_4-hBN (Hexagonal boron nitride) ceramic mixtures in artificial seawater when in contact with polyether-etherketone. Xu et al (2018) examined the tribological properties of polyphenylenesulphide (PPS) that was loaded with hydrolysable nanoparticles, specifically beta silicon carbide (SiC), hexagonal boron nitride (BN), or beta Si_3N_4 nanoparticles. Yin et al (2021) investigated the tribological characteristics of WC-TiC-Co–Ni (TiCN), WC-6Co (YG6X) and WC-6Ni (YN6X) cermets experience frictional interaction with SiC in seawater that was specially designed for the research. The findings indicated that the wear and friction characteristics of the tribopairs were improved as the sliding speed increased.

Wei et al (2022) evaluated the tribological characteristics of Si_3N_4 balls, which were manufactured using various sintering procedures and sintering components. They examined the performance against containing steel under circumstances involving extreme loads and high-frequency fretting while lubricated with lubricate. Wang et al (2022) executed friction tests using graphite powder, h-BN powder and MoS_2 powder at various temperatures and stages. Their study analyzed the tribological features and lubrication process. Kaushik and Ramkumar (2018) examined the tribological characteristics of bearing steel, Si_3N_4 and

zirconia while exposed to extreme temperatures and powerful engine oil SAE20W-40 lubricant. Si_3N_4 Outperformed steel and zirconia in terms of tribological efficiency. The tribological properties of a new 2D SiP lubricating material were initially evaluated in research (Yu et al 2022). The tribological characteristics of hexadecane in the presence of SiP nanoflakes were examined at various loads and concentrations. Huang et al (2022) described the fabrication process of composite coatings consisting of Ni/Si_3N_4. The procedure involved the electrophoretic deposition of Si_3N_4 particles followed by the electroplating of Ni coatings. The outcome demonstrated that low friction was not a distinctive characteristic of self-mated pairs of Si_3N_4 and SiC.

The subsequent portions of this study are organized as follows: Section 2- Materials and methods, Section 3- Result and Section 4- Conclusion.

2. Materials and methods

Three accessible lubricates were analyzed, each of them specifically developed for use in EM in accordance with the manufacturers' specifications. The mineral-polyurea (MPu), synthetic-lithium complex (SLi) and mineral-lithium (MLi) lubricates are the particular types examined. It should be noted that lubricates were assessed, easily accessible and specific information about their formulation, such as their composition as well as amount of components, was not recognized. Table 1 presents the recorded data regarding every lubricate.

Table 1EM lubricate parameters [Source: Author]

EM Lubricate	Acronym	BO Viscosity at 40 $°C$	Dropping Point (ASTM $D2265$ $°C$)	BO Density at 15 $°C$	BO Viscosity at 100 $°C$
Synthetic-lithium complex	SLi	100	260	0.85	14
Mineral-lithium	MLi	100	180	0.93	11
Mineral-polyurea	MPu	100	260	0.88	12

The EM lubricates' tribological efficiency was assessed through the conductance of two types of testing. Initially, a “Rtec Instruments Multi-Function Tribometer," was utilized for performing a one-way sliding “ball-on-disk test” (BODT), as depicted in Figure 1a. The experiments utilized a Si_3N_4 ceramic bearing ball measuring 9.525 mm in size and possessing an average SR (Ra) of s20 nm. The ceramic balls corresponded to the level 5 quality standards. The disk was a flat circular shape with a diameter of 50.8 mm. It was composed of toughened chrome steel. The disks were polished using an “Allied High Tech Metprep 3 polisher” and a SiC “abrasive pad” in a H_2O dispersion for irregular quality of the surface. A "Bruker DektakXT" profilometer operating in contact mode was used to assess the disks' SR. Before performing the tests, all the testing surfaces underwent ultrasonic

cleaning using heptane.

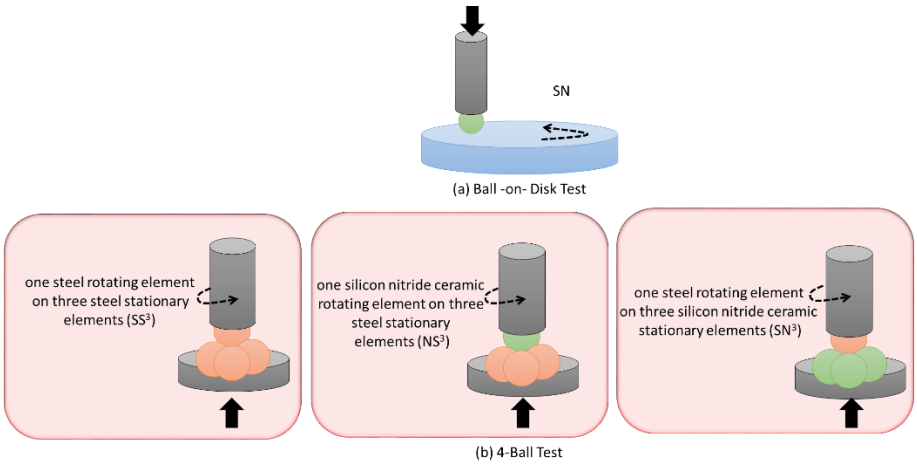

Figure 1(a-b)Two test settings were used to characterize lubricates

[Source: Author]

The specifications of the BODT were strictly followed according to the ASTM D5707-16 standard, with certain modifications made to account for important circumstances anticipated in EM environments. These changes focused on the SR, temperatures and bearing material. The applied force was 10 N, resulting in a high Hz "contact pressure (CP)" of 1.3Gpa. The velocity of sliding is 260 millimetres per second. The temperatures that had been tested were 40, 100 and 150 °C. Approximately 500 mm^3 of lubricate was used to lubricate the samples for every experiment. A "lubricate scoop" was utilized during assessment at a temperature of 40 °C to prevent lubrication scarcity by putting the lubricate back onto the track. The experiments were conducted with a total slide distance of 400 meters and every state of testing was performed 3 times.

Additionally, a "Falex Multi-Specimen Test Machine" was utilized to conduct a "4-ball test" (4-BT), as depicted in Figure 1b. The 4-BT facilitated the evaluation of various mixtures of Si_3N_4 and strengthened chrome steel. Three distinct material compositions underwent testing.

- A single steel rotating component is surrounded by three steel stationary elements (SS^3).
- The system consists of a single Si_3N_4 ceramic component and three stationary steel components (NS^3),
- A single steel rotating component supported by three stationary Si_3N_4 ceramic components (SN^3).

The SS^3 case exhibited the characteristics of a conventional all-steel bearing construction, while the NS^3 case displayed the features of a hybrid bearing system. The SN^3 is a reversed hybrid bearing assembly, utilizing conventional racing material as a rolling component. Its test specifications align with "ASTM-D2266 standard". The applied load was383 ± 3 N,

resulting in a high Hz CP of 4.7 GPa for the SS^3 established and 5.3 GPa for the NS^3/SN^3 combinations. The ceramic test balls, Si_3N_4, met grade 6 quality standards with a 20 nm SR, while the steel balls (SB) met grade 11 standards with a 26 nm SR. The speed was maintained at 1300 ± 90 turns per minute for duration of 90 min, while the temperature was maintained at $77\ °C \pm 3\ °C$. Each of the three lubricates performed testing with every material composition. The SS^3 and NS^3 results represent the average of three assessments, while the SN^3 results represent the maximum of two assessments. The error was determined by subtracting the minimum wear from the maximum wear for each arrangement and type of lubricate.

The wear volume for the BODT was determined using a Leica Optical Microscope and the worn ball surfaces were photographed for both testing methods. By employing the load's volume and the “total sliding distance," the wear rate (WR) was calculated. The “wear scar (WS)” dimensions were determined according to the ASTM D2266-01 standard for the 4-BT, the evaluations were utilized to measure the surface area of the scar.

3. Results and discussion

3.1 Ball-on-disk Friction

Figure 2 displays the friction values for every type of lubricate. The data in Figure 2a demonstrates that, on average, friction levels increase in correlation with the roughness of the surface for all types of lubricates. The MLi demonstrated a lower friction characteristic over rough surfaces (RSs). During the evaluations, it was observed that the lithium-based lubricates exhibited less friction compared to the “poly urea greases (PGs)," apart from the smooth surface (SS) where the “friction coefficient (FC)” was consistently < 0.09 for every types of lubricates.

The friction measured at three distinct temperatures is displayed in Figure 2b. At a temperature of $40\ °C$, the SP lubricate demonstrated the least amount of friction, whereas at a temperature of $100\ °C$, the SLi lubricate revealed the lowest level of friction. Synthetic greases (SGs) exhibited less friction than mineral greases (MGs) at both 40 and $100\ °C$. At a temperature of $160\ °C$, the FC exhibited similar values for all three lubricates.

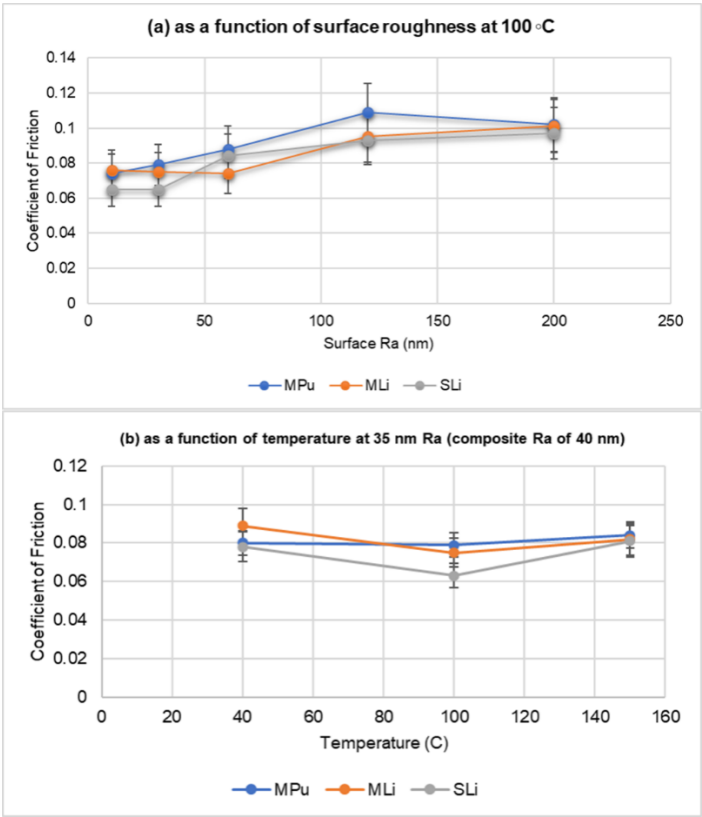

Figure 2(a-b)The friction outcomes of BODT [Source: Author]

The friction relationship between roughness and temperature is non-linear. The reason for this is due to the fact that temperature and SR have an impact on the lubrication condition. Moreover, a high temperature can enhance the occurrence of lubricate bleed, resulting in a decrease in the level of scarcity as the temperature rises. Therefore, an ordinary linear fit cannot be used to measure the impact of these characteristics on friction. Instead, will be covered later, these patterns will be examined in the framework of the Stribeck curve.

3.2 4-Ball Test (4-BT)

The results obtained from the 4-BT are displayed in Figure 3. MLi bearing design showed minimal wear due to thicker lubrication films and enhanced anti-wear development, offering greater distance between surfaces. Average wear for the SS^3 and NS^3 variants follows the pattern MLi $<$ MPu $<$ SLi. The 4-BT's antiwear performance is unclear due to unreport lubricate composition, high wear in the SN^3 arrangement and too many error bars for accurate assessment.

When evaluating various material combinations, it was found that NS^3 had the least average wear among all lubricates, subsequent to SS^3 and then SN^3. The finding that wear in NS^3 was reduced compared to SS^3 corresponds to prior studies indicating that the lifespan of lubricate in hybrid bearings is greater than that in conventional bearings. The reduced wear observed in the NS^3 is in accordance with anecdotal and empirical data indicating that hybrid bearings

have longer lifespans compared to what is predicted by the Lundberg-Palmgren equations.

However, the SN^3 design exhibited high wear. This arrangement displayed qualitatively distinct behaviour compared to the other two component pairs. The insets in Figure 3 demonstrate that the WSs of the SS^3 and NS^3 structures are circular, but the WSs of the SN^3 structures are oval. The wear process of the rotating parts determines and can result in non-circular WSs on the static balls. Hence, the difference might be attributed to the rigidity of the rotational component. In the case of SN^3, the SB serves as the rotating component that is connected to the spindle, whereas the three lower balls are made of Si_3N_4. The hardness of a material directly impacts its wear. When a softer SB rotates against a “harder ceramic ball," the WS on the surface of the ball becomes longer as the material changes. This leads to a separation between the lower and upper balls.

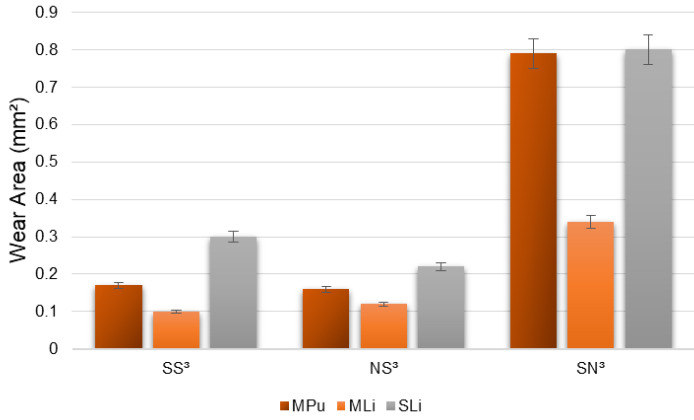

Figure 3The wear area results employing the 4-BT [Source: Author]

3.3 Ball-on-disk Wear

The relationship between SR and WR for every EM lubricates is depicted in Figure 4a. The WRs of the three lubricates are comparable on SS, with the MPu lubricate exhibiting the least wear. The MLi lubricate exhibits a low rate of wear on rougher surfaces, indicating greater distinction among lubricates. Furthermore, when considering these specific testing criteria, lubricates produced with mineral-based oil exhibit a reduced rate of wear compared to lubricate created with synthetic BO.

The relationship between roughness changes and WR was measured using a linear line slope, allowing easy comparison of lubricates based on WR growth. The slope derived from a linear analysis of the relationship between the roughness and WR data is depicted in Figure 4b. Based on this data, it can be determined that the WR is least influenced by SR when using the MLi lubricate. Furthermore, among lubricates that were evaluated those with mineral-based oil exhibit a lower relationship between wear and roughness compared to lubricate with synthetic BO.

The WRs corresponding to various temperatures are displayed in Figure 4c. At a temperature of 40 ℃, none of lubricates show any visible signs of wear. The MLi lubricate has the lowest WR at a temperature of 100 ℃, while the SLi lubricate demonstrates the lowest WR at a

temperature of 150 °C. Furthermore, at temperatures of 100 and 150 °C, the lithium-hardened lubricates in the examined samples exhibit a lower rate of wear compared to the PGs.

The temperature dependence of the rate at which wear occurs varies between synthetic and mineral-based lubricates. In particular, the rate at which wear occurs shows a constant value for SGs, while it increases in a straight line between temperatures of 100 and 150 °C for MGs. As a result of this behaviour, the linear approach is not suitable for measuring the alteration in WR with temperature for SGs. However, a linear regression analysis was conducted for the MGs, as depicted in Figure 4d. The WR of the MLi lubricate exhibits a lower degree of dependence on temperature compared to the MPu lubricate.

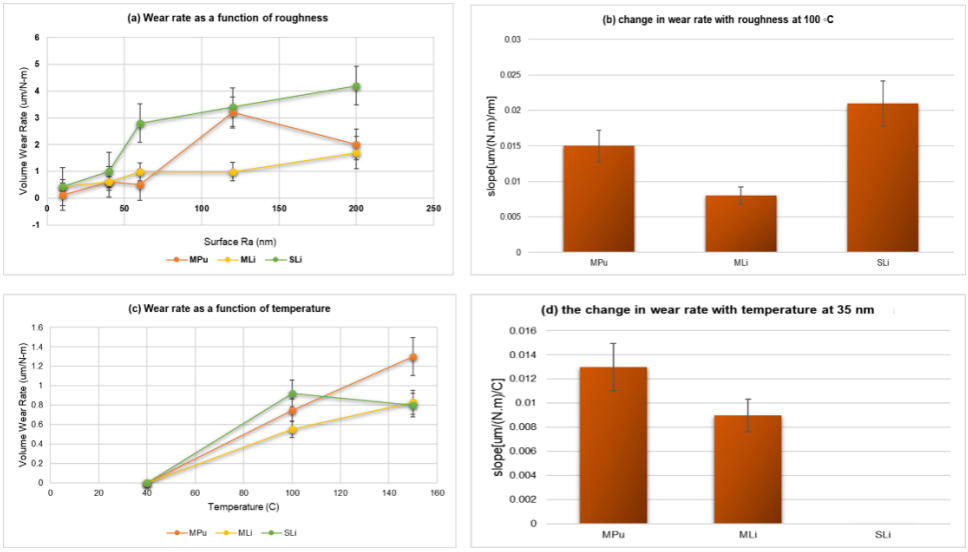

Figure 4(a-d)Outcomes obtained from EM lubricate BODT [Source: Author]

3.4 Analysis & Discussion

3.4.1 Grease Analysis

The research assessed the efficacy of three distinct lubricates under diverse SR and temperature settings, revealing varying levels of effectiveness. The following findings are explained below. MLi had the lower rate of wear on RSs, whereas MPu had the lower WR on SS, as shown in Figure 4a. It was discovered that MLi showed the least amount of WR dependent on SR. The roughness and WR dependence of mineral BO-based lubricates are lower than those of synthetic-based lubricates. SLi lubricate had a low WR in tests conducted at high temperatures (150 °C). Additionally, at high temperatures, the WR of the SGs remained constant, but the WR of the MGs increased with temperature. During the 4-BT, MLi exhibited the least amount of wear among all the different bearing designs. Regarding the SS^3 and NS^3 designs, the average wear experienced an increase in the following order MLi $<$ MPu $<$ SLi. Higher rates of wear result in increased production of material debris, which can lead to consequences such as the creation of an artificial RS, a decreased capacity to provide lubrication along with increased erosion and abrasion.

Therefore, minimizing wear is of utmost importance.

Considering friction, the SLi lubricate exhibited low friction on the majority of surfaces. On surfaces with more appearance, the lithium lubricates exhibited decreased friction compared to the PGs. On exceptionally SS, the synthetic substances exhibited reduced friction compared to lubricate derived from minerals. At a temperature of 100 ℃, the SLi lubricate exhibited a low level of friction. The study found that SGs had less friction than MGs at 40 and 100°C. MLi had the lowest λ_t value, indicating it maintained its FFR for longer. However, it increased friction in the transitional area, while SLi had a higher λ_t ratio but reduced friction.

While the evaluations of lubricate based on certain performance indicators are useful, it is necessary to integrate these comparisons to ascertain the optimal lubricate for a particular application. Hence, it is essential to develop a methodology for evaluating and comparing commercially accessible lubricates.

The performance measures considered in the study are low SR friction, low-temperature wear and friction, high SR wear and friction, high-temperature wear and friction, wear dependence on SR as well as NS^3 wear derived from the 4-BT. The ranking system was designed for applications involving EM bearings, prioritizing extreme temperatures, friction and wear by assigning them double the weight of other parameters. Lubricates were assigned numerical rankings from 1 to 3, with 3 indicating the highest quality. Figure 5 displays the results in the form of radar graphs.

The individual evaluations for each lubricate were combined to obtain a comprehensive score, which is displayed alongside the radar graph in Figure 5. The two lithium lubricates demonstrated superior performance compared to the PG, as indicated by the total score ($\mathrm{SLi} = 36 > \mathrm{MLi} = 33 > \mathrm{MPu} = 24$). The total score can be categorized into wear and friction ratings, both of which are displayed alongside radar graphs in Figure 5. The findings demonstrate that the SGs exhibited superior friction performance compared to the mineral-based lubricates ($\mathrm{SLi} = 20 > \mathrm{MLi} = 11 > \mathrm{MPu} = 8$). SLi demonstrated superior friction efficiency, especially at high temperatures, which was consistent with the overall grade. However, when it comes to wear, MGs have shown better performance compared to SGs. This is demonstrated by the total wear scores, with MGs scoring higher ($\mathrm{MLi} = 22 > \mathrm{SLi} = 16, \mathrm{MPu} = 16$). The MLi demonstrated superior wear performance, specifically showing a minimal correlation between wear and SR. MPu and SLi were regarded as the second-best, but SLi's high ranking was mainly because it had low wear at high temperatures. MPu performed better than SLi in all other measures of wear, especially in terms of wear on surfaces with low roughness.

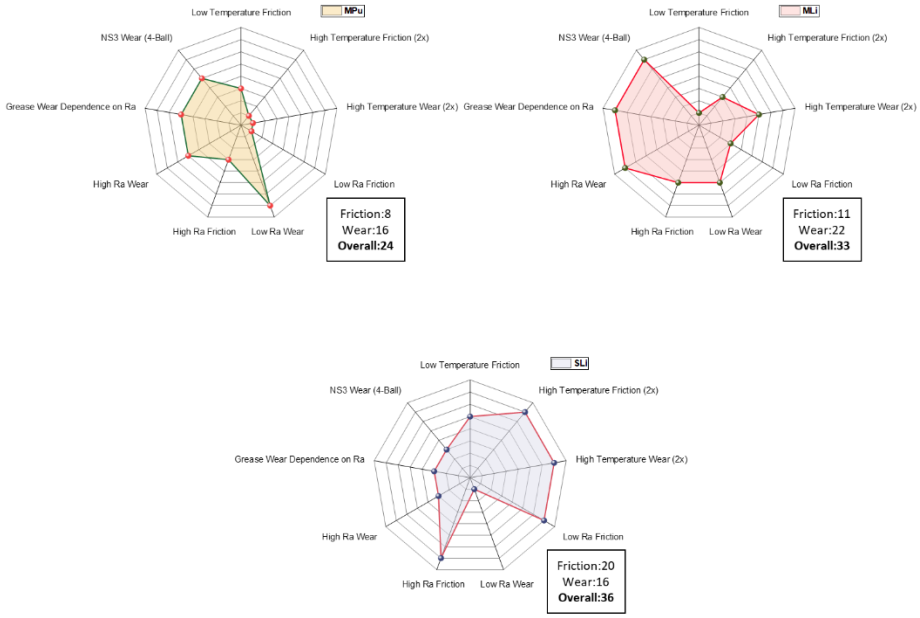

Figure 5Lubricate ranking method (1-3) [Source: Author]

Total ratings and radar graphs guide designers in assessing lubricates for specific applications, but long-term bearing/lubricate life studies are crucial for evaluating lubricate suitability for EM systems. Total ratings and radar graphs provide lubricate assessment for specific applications, but long-term lubricate/bearing life studies are crucial for evaluating lubricate suitability in EM systems.

3.4.2 Analysis of the lubrication regime

The friction outcomes in Figure 2 indicate that an adjustment in "roughness or temperature" was responsible for the change in lubrication conditions. The lambda ratio is used to determine the lubrication procedure, as shown in Equation (1).

$$\lambda = \frac{g}{(Ra_{ball}^2 + Ra_{disk}^2)1/2} \quad (1)$$

Where,

g - Thickness of the film,

Ra_{disk} - Average roughness (AR) of the disk,

Ra_{ball} - AR of the ball,

λ - Transitions between lubrication regimes,

$1 \leqq \lambda \geqq 3$ - mixed lubrication (ML),

$\lambda \geqq 3$ - Full film lubrication (FFL) and

$\lambda \leqq 1$ - Border lubrication.

Analysis shows FFL or ML can occur even in situations where the border lubrication

parameter λ indicates. The frictional fatigue life of bearings is influenced by the λ ratio. Surface displacement and distress are correlated with low λ ratios. Within the parameters examined in this study, it has been observed that surfaces with minimal roughness and lower temperatures, which result in greater λ ratios, exhibit reduced contact fatigue and extended lifespan. The "film thickness (FT)" of a lubricate coating was determined using the "Hamrock and Dowson" Equation (2), considering the specific values of the BO, to determine the value of λ.

$$g \approx g_d = 2.69R\left(\frac{V\eta}{ER}\right)^{0.67}(\alpha F)^{0.53}\left(\frac{X}{ER^2}\right)^{-0.067}\left(1-0.61f^{-0.73l}\right) \quad (2)$$

Where, α - Pressure-viscosity coefficient,

$l = 1$ - Spherical geometry,

E - Effective elastic modulus,

V - Speed,

X - Load,

R - Effective radius and

η - Ambient viscosity.

The majority of characteristics remain constant throughout BODT, but pressure-viscosity and ambient viscosity coefficient are determined by considering temperature and BO rheological characteristics. Table 2 presents the results of the FT and λ ratio for each combination of temperature, roughness and EM lubricate that were examined in this investigation.

Table 2EM Lubricate Evaluated the Lambda (λ) ratio and FT [Source: Author]

Temperature °C	Composite Roughness nm	MPu		MLi		SLi	
		h_c	λ	h_c	λ	h_c	λ
40.0	40.5	151.4	3.94	142.4	3.72	117.4	40.5
100.0	22.6	28.0	1.45	27.1	1.40	28.5	22.6
100.0	40.5	28.0	0.89	27.1	0.87	28.5	40.5
100.0	63.5	28.0	0.64	27.1	0.62	28.5	63.5
100.0	121.9	28.0	0.43	27.1	0.42	28.5	121.9
100.0	201.2	28.0	0.24	27.1	0.23	28.5	201.2
150.0	40.5	11.5	0.48	11.2	0.47	13.9	40.5

Figure 6 displays a Stribeck curve, which represents the relationship between the friction obtained from the BODT and the predicted λ ratio. The experiments conducted at lower temperatures and on SS are correlated with larger λ conditions. Lower λ ratios are caused by high temperatures and RSs. The "Stribeck curve" depicted in Figure 6 demonstrates the presence of the mixed regime, characterized by a reduction in friction with λ and the "full film regime (FFR)," characterized by a rise in friction with λ, in our testing.

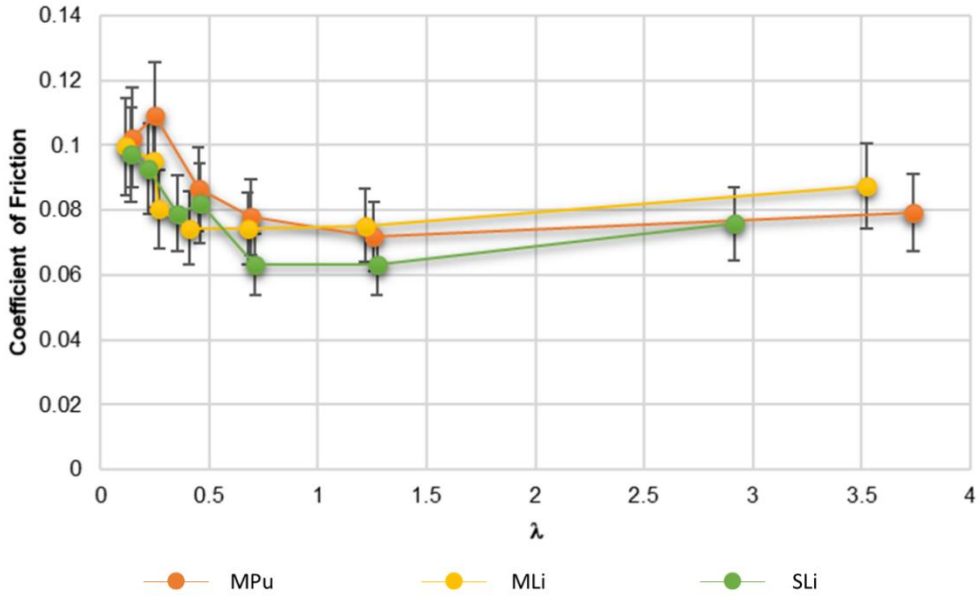

Figure 6Stribeck curve obtained by measuring friction and computing λ ratios [Source: Author]

Lubricates clearly demonstrate complete coverage at higher lambda ratios. The SLi demonstrated the least amount of friction in this particular scenario. The presence of a mixed regime is apparent when the λ ratios are low. As the level of composite roughness rises, the values of λ reduce, leading to a rise in friction. The MLi and SLi lubricates, which contain lithium thickener, exhibited the least amount of friction in ML. SLi exhibited superior friction performance throughout the majority of examined lubrication settings.

The transition from FFL to ML environment increases wear and friction due to harsh connections in the interface. It is recommended to persist in the FFL for as long as possible. The transition lambda (λ_t) represents the point of intersection between linear regression lines for each lubricate type, which is displayed in Figure 7.

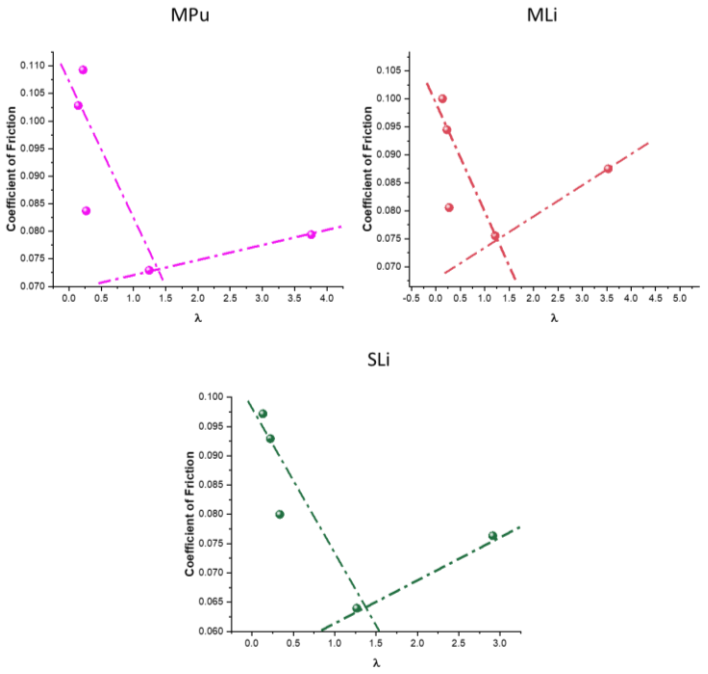

Figure 7Separate linear regression analyses were conducted for the mixed and FFR [Source: Author]

The $\lambda_t$values for each type of lubricate were determined as follows: MPu has a λ_t value of 0.47, MLi has a λ_t value of 0.37 and SLi has a $\lambda_t$value of 0.58. The MLi lubricate has a lower λ_t, suggesting it stays in the FFR for longer when "temperature or roughness" increases. However, it has increased friction. SLi has a higher λ_t but lower friction, indicating a compromise between achieving low friction and maintaining the interface's state before changing to ML.

4. Conclusions

The study conducted a complete evaluation of the efficiency of three accessible lubricates designed for EM purposes. The evaluation includes 4-ball and BODT to evaluate tribological efficiency across multiple situations, including varying temperatures and surface roughness. BOD friction tests showed a positive correlation between friction levels and SR across lubricates, with MLi lubricate having superior properties on RSs. The 4-BT revealed that MLi lubricate had the lowest wear rate among the two bearing models, with favourable outcomes, especially on RSs, influenced by material combinations and temperature. The study found that lithium-based lubricates. Specifically, SLi and MLi outperformed PGs in overall ratings, with SGs showing greater friction efficiency at higher temperatures. The SLi material showed minimal wear and low friction, with SGs having superior friction characteristics and MGs showing the most favourable wear performance, with MLi lubricate as the most effective. The limitations originate from the limited comprehension of difficult conditions, the possibility of wear in practical uses and the difficulties in maintaining

constant lubrication for the sliding of Si_3N_4 on steel surfaces. The future prospects involve performing extensive research on materials, exploring the uses of nanotechnology and developing novel lubricating techniques to improve the effectiveness of Si_3N_4 sliding on steel.

References

1. Chen W, Wang K, Gao Y, He N, Xin H and Li H (2018) Investigation of tribological properties of silicon nitride ceramic composites sliding against titanium alloy under artificial seawater lubricating conditions. International Journal of Refractory Metals and Hard Materials 76:204-213. DOI: 10.1016/j.ijrmhm.2018.06.011
2. Elsheikh A.H, Yu J, Sathyamurthy R, Tawfik M.M, Shanmugan S and Essa F.A (2020) Improving the tribological properties of AISI M50 steel using Sns/Zno solid lubricants. Journal of Alloys and Compounds 821:153494. DOI: 10.1016/j.jallcom.2019.153494
3. Guo P, Geng Z, Lu Z, Zhang G and Wu Z (2018) Probing the lubrication mechanism of rough diamond-like carbon films against silicon nitride under water. Tribology International 128:248-259. DOI: 10.1016/j.triboint.2018.07.030
4. He Q, Li A, Wang Z, Zhang Y, Kong L and Yang K (2018) Tribological behavior of ZnO-Si3N4 nanoparticles-based lubricating grease. Journal of Experimental Nanoscience 13:1:231-244. DOI: 10.1080/17458080.2018.1511923
5. Huang L, Dai Q, Huang W and Wang X (2022) Ni/Si3N4 composite coatings and their water lubrication behaviors. Applied Surface Science 572:151534. DOI: 10.1016/j.apsusc.2021.151534
6. Kaushik Y and Ramkumar P (2018) Effect of Elevated Temperature on Tribological Properties of Steel, Silicon Nitride and Zirconia Against Steel. Advanced Science Engineering and Medicine 10:3-4:434-439. DOI: 10.1166/asem.2018.2154
7. Kronberger M and Brenner J (2023) Tribocorrosive Aspects of Tungsten Carbide, Silicon Nitride, and Martensitic Steel under Fretting-like Conditions. Lubricants 11:5:195. DOI: 10.3390/lubricants11050195
8. Lee Y.S, Yamagishi S, Tsuro M, Ji C, Cho S, Kim Y and Choi M (2021) Wear behaviors of stainless steel and lubrication effect on transitions in lubrication regimes in sliding contact. Metals 11:11:1854. DOI: 10.3390/met11111854
9. Li F and Guo B (2018) Effect of different lubricants on microstructural and tribological properties of TC21 titanium alloy against Si3N4 under fretting–reciprocating sliding. Journal of Alloys and Compounds 743:576-585. DOI: 10.1016/j.jallcom.2018.01.177
10. Li H, Liu X, Zhang C, Jiao X, Chen W, Gao J and Zhong L (2022) Friction and Wear Properties of Silicon Nitride-Based Composites with Different hBN Content Sliding against Polyether-Etherketone at Different Speeds under Artificial Seawater Lubrication. Coatings 12:3:411. DOI: 10.3390/coatings12030411
11. Lin B, Ding M, Sui T, Cui Y, Yan S and Liu X (2019) Excellent water lubrication additives for silicon nitride to achieve superlubricity under extreme conditions. Langmuir 35:46:14861-14869. DOI: 10.1021/acs.langmuir.9b02337
12. Lin H, Yang M.S and Shu B.P (2020) Fretting wear behavior of high-nitrogen stainless bearing steel under lubrication condition. Journal of Iron and Steel Research International 27:849-866. DOI: 10.1007/s42243-020-00414-z
13. Wang W, Wen H, He N and Chen W (2018) Effect of load on tribological properties of silicon nitride/steel under rolling-sliding contact condition. Tribology International 125:27-38. DOI: 10.1016/j.triboint.2018.04.022

14. Wang Z, Li S, Sun J, Wang J, Zhang L, Wei C, Xia Z, Zhang X and Yang J (2022) Effect of powder lubrication on wear characteristics of silicon nitride during sliding at high temperature. Materials Research Express 9:4:046403. DOI: 10.1088/2053-1591/ac62b7
15. Wei W, Liang H, Su Y, Fan H, Song J, Li W, Hu L and Zhang Y (2022) Fretting damage behaviors of silicon nitride balls with different sintering aids and processes under grease lubrication. Tribology International 171:107572. DOI: 10.1016/j.triboint.2022.107572
16. Xu Y, Guo Y, Li G, Zhang L, Zhao F, Guo X, Dmitriev A.I and Zhang G (2018) Role of hydrolysable nanoparticles on tribological performance of PPS-steel sliding pair lubricated with sea water. Tribology International 127:147-156. DOI: 10.1016/j.triboint.2018.05.042
17. Yin F, Wang Y, Ji H, Ma Z and Nie S (2021) Impact of sliding speed on the tribological behaviors of cermet and steel balls sliding against SiC lubricated with seawater. Tribology Letters 69:1-16. DOI: 10.1007/s11249-021-01413-1
18. Yu T, Xu S, Wu Z and Wang D (2022) 2D SiP nanoflakes as new high-performance lubricant additive for steel/steel sliding contact. Tribology International 169:107467. DOI: 10.1016/j.triboint.2022.107467
19. Zhang J, Liu J, Wang Z, Chen W, Hu B, Zhang Y, Liao H and Ma S (2020) Tribological behavior and lubricating mechanism of Si3N4 in artificial seawater. Ceramics International 46:10:14361-14368. DOI: 10.1016/j.ceramint.2020.02.171
20. Zhang J, Wang Z, Chen W, Liao H, Zeng M and Ma S (2019) Wear in silicon nitride sliding against titanium alloy pairs at different loads under artificial seawater lubrication. Frontiers in Materials 6:155. DOI: 10.3389/fmats.2019.00155